

Published in final edited form as:

*Circ Res.* 2013 October 25; 113(10): 1169–1179. doi:10.1161/CIRCRESAHA.113.302302.

## Rejuvenation of Human Cardiac Progenitor Cells With Pim-1 Kinase

**Sadia Mohsin, Mohsin Khan, Jonathan Nguyen, Monique Alkatib, Sailay Siddiqi, Nirmala Hariharan, Kathleen Wallach, Megan Monsanto, Natalie Gude, Walter Dembitsky, and Mark A. Sussman**

San Diego Heart Research Institute and Biology Department, San Diego State University, CA (S.M., M.K., J.N., M.A., S.S., N.H., K.W., M.M., N.G., M.A.S.), and Sharp Memorial Hospital, San Diego, CA (W.D.)

### Abstract

**Rationale**—Myocardial function is enhanced by adoptive transfer of human cardiac progenitor cells (hCPCs) into a pathologically challenged heart. However, advanced age, comorbidities, and myocardial injury in patients with heart failure constrain the proliferation, survival, and regenerative capacity of hCPCs. Rejuvenation of senescent hCPCs will improve the outcome of regenerative therapy for a substantial patient population possessing functionally impaired stem cells.

**Objective**—Reverse phenotypic and functional senescence of hCPCs by ex vivo modification with Pim-1.

**Methods and Results**—C-kit-positive hCPCs were isolated from heart biopsy samples of patients undergoing left ventricular assist device implantation. Growth kinetics, telomere lengths, and expression of cell cycle regulators showed significant variation between hCPC isolated from multiple patients. Telomere length was significantly decreased in hCPC with slow-growth kinetics concomitant with decreased proliferation and upregulation of senescent markers compared with hCPC with fast-growth kinetics. Desirable youthful characteristics were conferred on hCPCs by genetic modification using Pim-1 kinase, including increases in proliferation, telomere length, survival, and decreased expression of senescence markers.

**Conclusions**—Senescence characteristics of hCPCs are ameliorated by Pim-1 kinase resulting in rejuvenation of phenotypic and functional properties. hCPCs show improved cellular properties resulting from Pim-1 modification, but benefits were more pronounced in hCPC with slow-growth kinetics relative to hCPC with fast-growth kinetics. With the majority of patients with heart failure

---

© 2013 American Heart Association, Inc.

Correspondence to Mark A. Sussman, PhD, Department of Biology, San Diego Heart Research Institute, San Diego State University, 5500 Campanile Dr, San Diego, CA 92182., heartman4ever@icloud.com.

The online-only Data Supplement is available with this article at <http://circres.ahajournals.org/lookup/suppl/doi:10.1161/CIRCRESAHA.113.302302/-/DC1>.

#### Disclosures

M.A. Sussman is supported by National Institutes of Health grants R01HL067245, R37HL091102, R01HL105759, R01 HL113656, R01 HL117163, and R01 HL113647. M. Khan is supported by American Heart Association (AHA) post doctoral award 11POST7370097. N. Hariharan is supported by AHA post doctoral award 12POST12060191. The other authors report no conflicts.

presenting advanced age, infirmity, and impaired regenerative capacity, the use of Pim-1 modification should be incorporated into cell-based therapeutic approaches to broaden inclusion criteria and address limitations associated with the senescent phenotype of aged hCPC.

## Keywords

aging; cell cycle proteins; heart failure; telomere lengthening

The long-held belief of the heart as post mitotic organ<sup>1</sup> has been toppled by demonstration of myocyte turnover throughout life<sup>2</sup> and the existence of adult cardiac progenitor cells. Human cardiac progenitor cells (hCPCs) are multipotent<sup>3</sup> and capable of forming the 3 requisite cardiogenic lineages needed to form myocardium.<sup>4</sup> hCPCs isolated from failing human hearts augment cardiac function and myocardial regeneration in the clinical setting after adoptive transfer into pathologically injured myocardial tissue as demonstrated in the Stem Cell Infusion in Patients with Ischemic Cardiomyopathy (SCIPIO) trial.<sup>5,6</sup> The SCIPIO phase I trial was designed primarily to address feasibility and safety end points rather than therapeutic benefit, making the observation of functional and structural improvement in patients even more remarkable. However, a significant unresolved issue in SCIPIO, as well as other early clinical trials for autologous cellular treatment of heart failure, is the relatively narrow inclusion/exclusion criteria of patient eligibility to participate. Concurrent presentation of heart failure with comorbidities of chronic disease (eg, diabetes mellitus, obesity, hypertension,), habitual stressors (eg, smoking, poor diet, alcoholism), or genetic predisposition contribute to impaired reparative capacity, leaving patients with such conditions with little hope to benefit from current gains in cellular regenerative therapy. The ability of hCPC to maintain cardiac repair is significantly compromised by several factors, including genetics,<sup>7</sup> progression and disease pathogenesis,<sup>8,9</sup> heart load,<sup>10</sup> medication, and aging.<sup>11,12</sup> Advanced age is a primary risk factor for developing heart failure, and hCPCs in aged patients with heart failure are characteristically senescent with limited replicative capacity blunting cellular replacement and accelerate the aging process caused by the accumulation of large and poorly contracting myocytes.<sup>11</sup>

Reparative ability of CPCs can be significantly enhanced by molecular interventional approaches to increase survival, proliferation, engraftment, commitment, and persistence.<sup>13,14</sup> Superior regeneration and functional improvement mediated by human CPCs modified with Pim-1 kinase relative to identically expanded but nonmodified CPCs were demonstrated using cells isolated from an aged patient with heart failure at the time of left ventricular assist device (LVAD) implantation in a murine myocardial infarction model.<sup>14</sup> Pim-1 kinase enhances proliferation,<sup>13</sup> metabolic activity,<sup>14</sup> differentiation<sup>15</sup> and involves in neovascuogenesis<sup>16</sup> and neomyogenesis that forms an integral part of cardiac repair and regeneration response. Pim-1 also serves as a prosurvival role by preserving mitochondrial integrity<sup>17,18</sup> and antagonizing intrinsic apoptotic cascades.<sup>19</sup> Moreover, Pim-1 preserves telomere length and telomerase activity consistent with a youthful cellular phenotype.<sup>14</sup> Although ex vivo genetic modification of hCPC to augment regenerative potential is a viable option, reproducibility of Pim-1-mediated cellular enhancement in the context of a heterogeneous patient population with heart failure remains to be demonstrated.

There is more to aging than the chronologic measure of time passage. Cellular aging is reflected by a constellation of molecular and phenotypic changes consistent with acquisition of senescence. Biological age of a cell is most commonly assessed by telomere length, which is affected by multiple factors, including mitotic activity, environmental stress, and genetic damage. Clear correlations between cardiovascular disease risk and telomere length highlight the importance of studying characteristics of biological aging on a molecular level to comprehend critical relationships between cellular phenotype, functional behavior, and preservation/restoration of myocardial health.<sup>20,21</sup> Shortening of telomeres is associated with cellular arrest, acquisition of a senescent phenotype, and even cell death<sup>22</sup> that all contribute to the loss of regenerative potential with age. Indeed, aging itself can be considered, in part, a stem cell-mediated disease.<sup>23</sup> The loss of regeneration and reparative capacity inevitably leads to inability to cope with chronic stress or acute pathological injury. Reduction in hCPC ability to repair myocardium attributable to patient age, and pathology represents a serious problem and needs to be addressed before extending the beneficial effect of hCPC-based cell therapy for the treatment of heart failure. Patients with heart failure requiring LVAD implantation represent the target population most likely to experience impaired adult hCPC functional capacity; therefore, this study focuses on characterization of cells isolated from these patients. Results shown here demonstrate that hCPC isolated from multiple patients with varying age and disease pathogenesis possess variable growth kinetics, telomere lengths, and concomitant differences in expression of senescence markers. hCPC carrying the cumulative effects of age and disease can be rejuvenated by modification with Pim-1 kinase and can be promoted to drive a youthful phenotype to antagonize characteristics of cellular senescence.

## Methods

### Human Cardiac Stem Cell Isolation

hCPCs were isolated from heart tissue obtained from patients undergoing surgery for LVAD implantation as described previously.<sup>14</sup> Briefly, tissue was minced in small pieces and digested in collagenase 150 U mg/mL (Worthington Bio Corp, Lakewood, NJ) for 2 hours at 37°C. Cells were incubated with c-kit-labeled beads (Miltenyi Biotec, St Auburn, CA) and sorted according to the manufacturer's protocol. The pellet was suspended in hCPC media: Hams F12 (Fisher Scientific), 10% FBS, 1% PSG, 5 mU/mL human erythropoietin (Sigma Aldrich), 10 ng/mL basic FGF (Peprotech), and incubated at 37°C in CO<sub>2</sub> incubator. Adherent cells were seeded and expanded clonally. C-kit expression in hCPC is 87% to 89% measured by fluorescence activated cell sorting analysis (Online Figure IA). hCPC from multiple patients showed differences in growth kinetics. Two hCPC lines with distinct proliferation potentials were chosen for further experiments. H10-004 exhibited the slowest growth rate and is referred to as hCPC-S, whereas H10-014 exhibited the fastest growth rate referred to as hCPC-F. Fetal CPCs were isolated from fetal heart samples (second trimester) obtained from Novogenix laboratories.

### Generation of Lentiviral Vectors and Transduction of hCPC

hCPCs expressing enhanced green fluorescent protein (hCPC-eGFP) and hCPC-Pim were transduced with lentivirus for eGFP and Pim-1 and eGFP as previously described.<sup>14</sup> hCPC-S

and hCPC-F were modified with lentiviral vectors Lv-eGFP and Lv-eGFP+Pim1 (Online Figure IB), and efficiency of modification after lentiviral transduction was 77.1% and 79.4% with Lv-eGFP and Lv-eGFP +Pim, respectively, as measured by flow cytometric analyses for eGFP (Online Figure IC). Pim-1 overexpression in hCPC was confirmed by immunoblot analysis (Online Figure ID).

### Real-Time Reverse Transcriptase-Polymerase Chain Reaction

Total RNA was isolated from hCPC and treatment using Quick-RNA MiniPrep (Zymo Research) according to manufacturer's protocol. cDNA was prepared using iScript cDNA Synthesis Kit (Bio Rad). Real-time polymerase chain reaction (PCR) was performed on samples in triplicate using iQ SYBER Green (Bio Rad). Primer sequences are listed in Online Table I.

### Protein Isolation and Immunoblot Analysis

hCPC were plated in 6-well dishes (50 000 cells/well). Samples were harvested in 50  $\mu$ L of sample buffer, boiled, and sonicated. Protein lysates were run on 4% to 12% NuPage Novex Bis Tris gel (Invitrogen), transferred on to a polyvinylidene fluoride (PVDF) membrane, blocked in 8% skim milk in Tris-buffered saline Tween-20 solution for 1 hour at room temperature, and then incubated with primary antibodies overnight at 4°C. Membrane was incubated with secondary antibodies for 1 hour at room temperature after several washes with Tris-buffered saline Tween-20 solution. Fluorescence signal was detected and quantified using Typhoon fluorescent scanner together with Image Quant 5.0 software (Amersham Biosciences). Antibodies are listed in Online Table II.

### CyQuant, Viability, and MTT Assays

CyQuant assay involves plating cells in quadruplicate (2000 cells/ well) in a 96-well plate and incubation with MTT reagent (Sigma Aldrich) or CyQuant reagent (Life Technologies) as previously described.<sup>13</sup> Viability assay was measured by trypan blue staining.<sup>13</sup> Population doubling times were calculated using reading from CyQuant and viability assays and a population doubling time online calculator (<http://www.doubling-time.com/compute.php>).

### Cell Death Assay

hCPC were plated in a 6-well dish (30 000 cells/well) and incubated in hCPC medium with 2.5% serum overnight and then treated with 30  $\mu$ mol/L H<sub>2</sub>O<sub>2</sub> for 3 hours the following day. Cell death was confirmed by visualizing the cells under a light microscope before collection. Cells were harvested and stained with Annexin-V (Life Technologies) according to manufacturer's protocol. Data were acquired with the BD fluorescence activated cell sorting Canto and analyzed by Flow Jo or fluorescence activated cell sorting Diva software (BD Biosciences).

### Telomere Length Measurement (Quantitative Fluorescence In Situ Hybridization)

Telomere length was analyzed by quantitative fluorescent in situ hybridization (quantitative fluorescence in situ hybridization) and confocal microscopy. PNA probe (Dako) was used to

label telomeres according to manufacturer's protocol. Telomere staining was scanned using Leica LCS confocal and relative fluorescent unit was measured by Leica LCS software. To control for experimental variation, all experimental slide sets were scanned using identical settings on the confocal microscope. A minimum of 200 hCPC were analyzed per line.

### **Telomere Repeat Amplification Protocol Assay**

Telomerase activity was assessed by telomere repeat amplification protocol assay using quantitative PCR according to the manufacturer's protocol (TRAPeze RT; Chemicon S7710) and as described in the Materials in the Online Data Supplement.

### **Telomere Length Measurements (RT-PCR)**

Telomere length was measured by real-time PCR detection system by modified monochrome multiplex quantitative PCR method as described previously.<sup>24</sup> In a duplex PCR detection method, albumin was simultaneously amplified with telomere template to normalize for different amounts of DNA per well and sample. The detailed protocol and thermal cycling profile are described in the Materials in the Online Data Supplement.

### **Senescence-Associated $\beta$ -Galactosidase Staining**

hCPC were cultured in 2-chamber permanox slides, and senescent cells were detected using a senescence-associated  $\beta$ -galactosidase assay (Abcam #ab65351) according the manufacturer's protocol. Images were obtained using Olympus IX70 microscope.

### **Measurement of Cell Morphology**

hCPC were plated in a chamber slides, and images were obtained using Olympus IX70 microscope. Cell morphology was measured by tracing the outline of the cells using ImageJ software. Twenty different fields of view were used to quantify cell morphology per cell line.

### **Statistical Analysis**

All data were expressed as a mean $\pm$ SEM. Comparison between 2 groups was performed using Student *t* test or multiple groups by 1- or 2-way ANOVA. *P* value <0.05 was considered as statistically significant. Statistical analysis was performed using GraphPad prism version 5.0 software.

## **Results**

### **Characterization of hCPC Isolated From Multiple Patients**

hCPC were isolated from multiple patients undergoing LVAD implantation. Population doubling times ranging from 28.1 to 21.5 hours were observed in the hCPC-S versus hCPC-F lines, respectively, as calculated by population doubling time. Growth kinetics are 30% faster in hCPC-F as compared with hCPC-S measured by population doubling time (Figure 1A; *P*<0.05). Growth rate of the hCPC-F is similar to the 21.2-hour doubling time for fetal CPC used as a standard control of healthy stem cells (Figure 1A). Similarly, increased proliferation rates were also observed using a CyQuant DNA labeling assay, with hCPC-F

exhibiting 60% and 90% greater labeling than hCPC-S, respectively (Figure 1B;  $P<0.05$ ). Similarly, 55.2% increase in telomere length was observed in hCPC-F as compared with hCPC-S (Figure 1C;  $P<0.01$ ). Telomere length measurements in hCPC showed variation from 2.1 kbp observed in hCPC-S to 3.8 kbp measured in hCPC-F. Telomere length in fetal CPC is substantially longer than adult CPC lines at 8.3 kbp (Figure 1C). Telomere lengths were measured at passage 6 in hCPC lines and fetal CPC. Increased cell death was observed in hCPC-S (26.6%) compared with hCPC-F (21%) after apoptotic stimulation (Figure 1D;  $P<0.05$ ). Fetal CPC exhibited 19.5% susceptibility to apoptotic challenge (Figure 1D). Collectively, these results indicate that concomitant changes in telomere length, population doubling time, and proliferation rates in hCPC can be used as readout for biological age of hCPC. Patient characteristics, including medical procedures, history, and medication, are listed in the Table. The limited sample number of the population precludes a correlative analysis between patient pathogenesis and hCPC characteristics, but it is worthy of note that hCPC-S is derived from a patient with concurrent comorbidities of diabetes mellitus and decades of chronic cigarette smoking, which may contribute to the relatively poor performance because hCPC-S is comparable with hCPC-F in chronologic age. However, small sample size of our study prevents drawing any firm conclusions for the underlying cause(s) of variability until additional samples and a larger population of hCPC isolates are characterized.

### Cell Cycle Regulator Profile in Human CPC

Profiling of cell cycle inhibitors, such as p16 and p53, was assessed by quantitative PCR analyzed in multiple hCPC lines. Transcript level increases of p53 ( $P<0.01$ ; Figure 2A) and p16 ( $P<0.05$ ; Figure 2C) were elevated in hCPC-S relative to hCPC-F as evidenced by lower CT values (CT values are inversely proportional to mRNA levels). Also, diminished p53 expression and the absence of detectable p16 signal was observed in fetal hCPC (Figure 2A and 2C). mRNA level differences coincide with changes in protein expression, with significant increases of both p53 (3.2-fold;  $P<0.001$ ) and p16 (2.1-fold;  $P<0.05$ ) in hCPC-S relative to hCPC-F, whereas lowest expression was consistently observed in fetal CPC as confirmed by immunoblot analysis (Figure 2B–2D). Proliferative markers were higher in hCPC-F versus hCPC-S as evidenced by increases in mRNA for Cyclin D1 ( $P<0.01$ ; Figure 2E) and Pim-1 ( $P<0.001$ ; Figure 2G) when comparing hCPC-F with hCPC-S, respectively. Increased mRNA of Cyclin D1 and Pim-1 is evidenced by lower CT values in hCPC-F as compared with hCPC-S. Concomitantly, increased protein expression of Cyclin D1 is observed in hCPC-F compared with hCPC-S (2.1-fold;  $P<0.001$ ; Figure 2F). Increased Pim-1 expression is observed in hCPC-F compared with hCPC-S as evidenced by immunoblot analysis (2.4-fold;  $P<0.05$ ; Figure 2H). Fetal CPC showed highest expression for both Cyclin D1 and Pim-1 (Figure 2F and 2H). Collectively, these results demonstrate the inherent variability between multiple hCPC lines with respect to expression of phenotypic markers indicative of senescence and proliferative status, both of which correlate with the biological properties of the cells in vitro (Figure 1).

### Replicative Senescence in Human CPC

Replicative senescence indicative of lowered proliferative potential was evident in hCPC-S compared with hCPC-F, with increased senescence-associated  $\beta$ -galactosidase-positive cells

after serial passaging (Figure 3A). hCPC-S acquired  $\beta$ -gal<sup>+</sup> expression at a higher rate than hCPC-F by passage 7 (63.3% versus 24.3%, respectively), whereas control fetal hCPCs were only 5.6%  $\beta$ -galactosidase positive at the same passage number ( $P<0.001$ ; Figure 3B). Subsequent passage-induced mitotic arrest was reached at passage 9 for hCPCs-S with 61.9% more  $\beta$ -gal<sup>+</sup> cells compared with hCPC-F (at passage 9), as hCPC-F continued to proliferate until passage 15 (Figure 3C). Acquisition of  $\beta$ -gal<sup>+</sup> expression indicative of senescence coincides with morphometric changes in hCPC. Specifically, hCPC-S become flat and lose normal morphology before mitotic arrest quantitated as decrease in length:width ratio ( $P<0.001$ ; Figure 3D) and increase in cell roundness ( $P<0.01$ ; Figure 3E) at passage 9 compared with hCPC-F. Taken together, these results are consistent with hCPC-S predisposition toward replicative senescence indicative of mitotic exhaustion caused by biological aging (as shown in Figures 1 and 2).

### Increased Telomere Length and Tert Activity in Pim-1–Modified hCPC

Variation in hCPCs as evidenced by proliferative capacity, replicative senescence, and telomere length (Figures 1–3) prompted further studies to assess reversibility of biological age and to drive youthful phenotypic characteristics. Previous studies by our group have demonstrated the ability of Pim-1 kinase to enhance myocardial regeneration<sup>13,14</sup> and to increase transiently telomere length.<sup>25</sup> In addition, Pim-1 kinase expression is higher in fetal hCPCs and hCPC-F compared with hCPC-S (Figure 2), establishing a correlation between Pim-1 expression and youthful phenotypic characteristics of hCPCs. On the basis of these results, we performed the genetic modification of hCPC-S and hCPC-F to overexpress Pim-1 kinase with subsequent analysis of telomere length and Tert activity. Pronounced white foci indicative of extended telomere length were observed in Pim-1–modified hCPC by quantitative fluorescence in situ hybridization analysis (Figure 4A and 4E) and are represented as relative fluorescent unit. Telomere length was significantly increased by 70% ( $P<0.001$ ; Figure 4B) in Pim-1–modified hCPC-S compared with hCPC-F (30%;  $P<0.01$ ; Figure 4F) when both cell lines were compared with respective control eGFP-modified hCPC. Quantitative fluorescence in situ hybridization was corroborated by PCR-based assessment of telomere length, showing a 2.2-fold increase in telomere length with Pim-1–modified hCPC-S ( $P<0.001$ ; Figure 4C) and 1.3-fold telomere length increase in Pim-1–modified hCPC-F ( $P<0.01$ ; Figure 4G) relative to respective eGFP controls. Similarly, a nonsignificant increase in telomere repeat amplification protocol activity is observed after Pim-1–modified hCPC-S (Figure 4D) and hCPC-F (Figure 4H) relative to respective eGFP controls. Collectively, these data indicate that Pim-1 modification elongates telomere length and promotes a youthful phenotype in hCPC, with greater enhancement of hCPCs possessing advanced biological age characteristics.

### Increased Proliferation, Metabolic Activity, and Survival After Pim-1 Modification

Genetic modification with Pim-1 significantly decreased population doubling time by 1.3-fold in hCPC-S ( $P<0.001$ ) compared with 1.1-fold decrease in hCPC-F ( $P<0.05$ ; Figure 5A). Concurrently, proliferation rate increased by 1.4-fold in hCPC-S ( $P<0.001$ ) and 1.2-fold ( $P<0.05$ ) in hCPC-F after Pim-1 modification with respect to eGFP-modified hCPC control as determined by CyQuant assay. Increased metabolic activity was exhibited by Pim-1–modified hCPC-S (30.7% higher) and hCPC-F (13.9% higher) compared with eGFP controls

at day 3 as measured by MTT assay (Figure 5C). Similarly, enhanced survival was demonstrated in Pim-1–modified hCPC-S and hCPC-F in response to apoptotic challenge as evidenced by respective decreases of 1.4-fold ( $P<0.01$ ) and 1.6-fold ( $P<0.001$ ) in Annexin-V+ cells (Figure 5D).

### Reversal of Senescent Phenotype After Ex Vivo Gene Manipulation With Pim-1 in hCPC

Senescence-associated  $\beta$ -galactosidase–positive staining was decreased after Pim-1-modification in hCPC-S (32.9%;  $P<0.001$ ) and hCPC-F (23.5%;  $P<0.01$ ; Figure 6A). Decreases in both cell length:width ratio and roundness indicative of cell flattening and a postmitotic phenotype were most prominently displayed in hCPC-S by passage 9 (Figure 6B and 6C) at which point the cells were no longer capable of further passaging because of loss of mitotic activity. In comparison, hCPCs-F maintain mitotic phenotypic properties at passage 9 and are capable of expansion until passage 14, indicating delayed senescence relative to hCPC-S. Restoration of growth-associated–rounded morphology to hCPC-S was conferred by Pim-1 modification that extended hCPC-S growth from passage numbers 9 to 15 before mitotic arrest (Figure 6D). Similarly, increased time in culture expansion was conferred by Pim-1 modification of hCPC-F from 14 to 19 passages before mitotic arrest (Figure 6D). In comparison, robust growth of fetal hCPCs used as the standard control for a youthful phenotype is capable of achieving passage 18 until growth arrest (Figure 3C) that compares favorably with the passaging limits of Pim-1–modified hCPC-F (19 passages) and hCPC-S (14 passages). p53 expression was decreased by 2.2-fold after Pim-1 modification in hCPC-S and lowered by 1.1-fold in Pim-1–modified hCPC-F. Similarly, p16 gene expression was calculated to be decreased by 3.5-fold by Pim-1 modification of hCPC-S and 1.3-fold by Pim-1 modification of hCPC-F (Figure 6E–6F). Collectively, the findings of Pim-1 modification indicate reversion of the aging phenotype for hCPCs. Moreover, with prior findings of telomere elongation (Figure 4), increased proliferation, and survival (Figure 5), the reversal of senescent phenotype supports a central role for Pim-1 in hCPC rejuvenation, particularly in hCPC compromised by biological aging.

### Discussion

Stem cell therapy for cardiac repair holds great promise, but the ability of cardiac stem cells to repair damaged myocardium declines with age.<sup>26–28</sup> Ex vivo expansion of hCPCs from pathologically challenged hearts is required in autologous therapy to expand the stem cell pool and select for proliferative cells before reinfusion, but in vitro demands on cell proliferation may exhaust the mitotic potential of isolated cells and may render them predisposed to undergo replicative senescence and compromised functional impact. Shortening of telomere length has been linked to both senescence<sup>21</sup> and cell death, further highlighting concerns related to expansion of hCPCs with telomeres compromised by aging and pathological stress. Heterogeneous origin of disease pathologies along with differences in individual genetic<sup>7</sup> and environmental makeup can adversely affect cardiac stem cell efficiency to repair damaged myocardium, limiting the beneficial effect of stem cell therapy. hCPCs derived from patients with advanced biological age and severe concurrent clinical features will require rejuvenation to reverse the deleterious effects of aging and disease. Findings in this study demonstrate that hCPCs isolated from multiple patients with heart

failure exhibit clear differences in growth rates, telomere lengths, and expression of senescent markers, representing biological age rather than chronological age as a key determinant of cellular phenotype. Genetic modification with Pim-1 kinase exhibits remarkable capacity to rejuvenate hCPCs with advanced biological age with enhanced proliferation, increased telomere lengths, and decreased susceptibility to replicative senescence. Telomere lengths of the 2 hCPC lines modified with Pim-1 were significantly longer, supporting the functional capacity of Pim-1 to reverse the phenotype of biological age in hCPCs. Pim-1 modification is a novel and effective way to augment hCPC function, extending the benefits of autologous stem cell therapy for the repair of damaged hearts to a large segment of the population with dissimilar age<sup>29</sup> and disease pathogenesis.

Myocardial repair processes in the heart are supported by CPCs located within cardiac niches.<sup>8</sup> Many intrinsic and extrinsic factors regulate CPC turnover and replenishment within the niche,<sup>30</sup> thus affecting CPC reparability in response to myocardial injury.<sup>27</sup> Accumulation of age-related changes,<sup>31</sup> such as DNA damage, telomere attrition,<sup>32,33</sup> epigenetic dys-regulation, and environmental stress, impair CPC function in the heart.<sup>34</sup> Heart-related pathologies primarily occur in the aged population<sup>35</sup> and compromise repair capability of endogenous CPC pool. Senescent CPCs are limited in their capacity to expand and to generate de novo cardiomyocytes, resulting in diminished cell turnover and acceleration of myocardial aging.<sup>36</sup> Indeed, CPCs isolated from multiple patients with varying age and disease pathologies have varying growth kinetics, telomere length (Figure 1), and expression of cell cycle regulators (Figure 2). However, telomere lengths from fetal CPC are the longest, and there is a clear distinction between the telomere length of samples derived from patients with LVAD and those derived from fetal samples. In addition to the chronological age, patients with heart failure display distinct disease pathogenesis and a combination of genetic and environmental factors that can impact CPC function. Analysis of patient characteristics and their respective CPCs revealed fast-, medium-, and slow-growing CPCs with growth rates inversely related to expression of senescent markers (Figure 2). hCPCs examined from patients with heart failure represent the target population that would benefit most from regenerative cell therapy, yet all of the samples analyzed fell short of exhibiting phenotypic characteristics comparable with fetal hCPCs used as the gold standard of a cardiogenic cell. The choice of fetal hCPCs for comparison was based on the rationale that the rapidly developing and highly mitotic environment of the fetal heart represents the characteristic regenerative potential desired with an adoptively transferred cell population intended to form myocardium. Ideally, the goal would be to introduce cells with maximal regenerative potential similar to a fetal cell with minimal risk for oncogenic transformation as is inherent with iPS or embryonic stem cell approaches. The fetal CPCs exhibit replicative senescence in culture at 19 passages, which was markedly prolonged relative to any of the hCPC patient-isolated lines without genetic modification to express Pim-1 kinase.

hCPCs for autologous therapy will depend on expansion of patient-derived cells in vitro, which expose hCPCs to the detrimental effects of high-pressure mitotic growth and concomitant replicative senescence and senescent characteristics (Figure 3). The capacity of Pim-1 kinase to enhance myocardial regeneration together with improved CPC survival, proliferation, and commitment to cardiac lineages has been demonstrated.<sup>13,15</sup> Furthermore, Pim-1 modification augmented telomere length and cell doubling time transiently in aged

murine CPCs.<sup>14</sup> However, in our initial study, we selected a hCPC line for adoptive transfer based on maximal expression of Pim-1 but had not addressed the potential for Pim-1 modification to result in varying outcomes based on the biological age of patient hCPCs. Although encouraged by our initial study with Pim-1–engineered hCPCs, the question of how broadly applicable this modification strategy remained unanswered and was highlighted in an editorial accompanying the article.<sup>37</sup> This subsequent report advances initial findings by showing beneficial effects of Pim-1 modification evident in divergent hCPC populations with varying phenotypes isolated from multiple patients. The present study performed an unbiased sampling of tissue samples from LVAD recipients, isolated their hCPCs, and then chose the cells with the hCPC-F and hCPC-S growth kinetics to represent the widest possible variation in phenotype as a platform for Pim-1 modification for rejuvenation of cells. Salutary effects of Pim-1 modification on proliferation (Figure 5) and telomere lengths (Figure 4) were consistent with suppression of p53 and p16 and blunting of the senescent phenotype (Figure 6). Importantly, Pim-1 modification exhibited beneficial effects in fast- and slow-growing hCPCs, the maximum increase in proliferation and telomere lengths was observed in slow-growing hCPCs, supporting the postulate that Pim-1 modification enhances phenotypic youthfulness in hCPCs regardless of initial differences in age or comorbidities. Indeed, the greatest benefit was observed in hCPCs isolated from patients that displayed advanced aging and the worse clinical features. Last, but not least, Pim-1 modification evoked a response consistent with restoring the hCPCs to a young phenotype but is capable of undergoing replicative senescence in a time frame comparable with the fetal hCPCs rather and did not exhibit a transformed behavior that would be unacceptable for clinical therapeutic use.

Clinical trials for heart repair have recently shown that hCPCs from patients are capable of mediating increases in ejection fraction and reducing scar size.<sup>5,6</sup> However, narrow inclusion criteria in these trials leave this question for debate whether initial beneficial results with hCPC transplantation are only applicable to a limited patient population with heart failure. Patients with heart failure show remarkable diversity in the pathogenesis of the disease. Various factors ranging from diabetes mellitus,<sup>38</sup> hypertension, smoking, stress, and life choices compound disease pathology. Importantly, incidence of heart failure coincides with increased age that further contributes to development of heart failure. Prerequisite for a successful, broadly applicable cell-based therapy for the repair of damaged myocardium demands a wide spectrum strategy to reduce the deleterious effects of aging, disease pathologies, and environmental factors. Pim-1 modification of age-exhausted or senescent hCPCs rejuvenates the phenotypic characteristics of the cells and accounts for our previous findings demonstrating the superior regenerative potential of Pim-1–engineered cells.<sup>13,14</sup> Modification of hCPCs by Pim-1 kinase is a viable strategy to rejuvenate hCPCs isolated from a diverse population with heart failure, opening up the possibility of extending hCPC-based cell therapy for the treatment of heart failure in a large segment of patients from various forms of cardiovascular disease.

## Supplementary Material

Refer to Web version on PubMed Central for supplementary material.

## Acknowledgments

We thank all members of the Sussman laboratory for their helpful discussions and San Diego State University FACS core facility for technical support.

## Nonstandard Abbreviations and Acronyms

<b>hCPCs</b>	human cardiac progenitor cells
<b>hCPCs-eGFP</b>	human cardiac progenitor cells expressing enhanced green fluorescent protein
<b>hCPCs-F</b>	fast-growing human cardiac progenitor cells
<b>hCPCs-Pim</b>	Pim-1–modified human cardiac progenitor cells
<b>hCPCs-S</b>	slow-growing human cardiac progenitor cells
<b>LVAD</b>	left ventricular assist device

## References

1. Anversa P, Leri A, Kajstura J. Cardiac regeneration. *J Am Coll Cardiol*. 2006; 47:1769–1776. [PubMed: 16682300]
2. Kajstura J, Gurusamy N, Ogórek B, et al. Myocyte turnover in the aging human heart. *Circ Res*. 2010; 107:1374–1386. [PubMed: 21088285]
3. Beltrami AP, Barlucchi L, Torella D, Baker M, Limana F, Chimenti S, Kasahara H, Rota M, Musso E, Urbanek K, Leri A, Kajstura J, Nadal-Ginard B, Anversa P. Adult cardiac stem cells are multipotent and support myocardial regeneration. *Cell*. 2003; 114:763–776. [PubMed: 14505575]
4. Dawn B, Stein AB, Urbanek K, et al. Cardiac stem cells delivered intravascularly traverse the vessel barrier, regenerate infarcted myocardium, and improve cardiac function. *Proc Natl Acad Sci USA*. 2005; 102:3766–3771. [PubMed: 15734798]
5. Bolli R, Chugh AR, D'Amario D, et al. Cardiac stem cells in patients with ischaemic cardiomyopathy (SCIPIO): initial results of a randomised phase 1 trial. *Lancet*. 2011; 378:1847–1857. [PubMed: 22088800]
6. Makkar RR, Smith RR, Cheng K, Malliaras K, Thomson LE, Berman D, Czer LS, Marbán L, Mendizabal A, Johnston PV, Russell SD, Schuleri KH, Lardo AC, Gerstenblith G, Marbán E. Intracoronary cardiosphere-derived cells for heart regeneration after myocardial infarction (CADUCEUS): a prospective, randomised phase 1 trial. *Lancet*. 2012; 379:895–904. [PubMed: 22336189]
7. Yao YG, Ellison FM, McCoy JP, Chen J, Young NS. Age-dependent accumulation of mtDNA mutations in murine hematopoietic stem cells is modulated by the nuclear genetic background. *Hum Mol Genet*. 2007; 16:286–294. [PubMed: 17185390]
8. Frati C, Savi M, Graiani G, et al. Resident cardiac stem cells. *Curr Pharm Des*. 2011; 17:3252–3257. [PubMed: 22114897]
9. Leonardini A, Avogaro A. Abnormalities of the cardiac stem and progenitor cell compartment in experimental and human diabetes. *Arch Physiol Biochem*. 2013
10. Kurazumi H, Kubo M, Ohshima M, Yamamoto Y, Takemoto Y, Suzuki R, Ikenaga S, Mikamo A, Udo K, Hamano K, Li TS. The effects of mechanical stress on the growth, differentiation, and paracrine factor production of cardiac stem cells. *PLoS One*. 2011; 6:e28890. [PubMed: 22216136]
11. Torella D, Rota M, Nurzynska D, Musso E, Monsen A, Shiraishi I, Zias E, Walsh K, Rosenzweig A, Sussman MA, Urbanek K, Nadal-Ginard B, Kajstura J, Anversa P, Leri A. Cardiac stem cell and myocyte aging, heart failure, and insulin-like growth factor-1 overexpression. *Circ Res*. 2004; 94:514–524. [PubMed: 14726476]

12. Anversa P, Rota M, Urbanek K, Hosoda T, Sonnenblick EH, Leri A, Kajstura J, Bolli R. Myocardial aging—a stem cell problem. *Basic Res Cardiol*. 2005; 100:482–493. [PubMed: 16237507]
13. Fischer KM, Cottage CT, Wu W, Din S, Gude NA, Avitabile D, Quijada P, Collins BL, Fransioli J, Sussman MA. Enhancement of myocardial regeneration through genetic engineering of cardiac progenitor cells expressing Pim-1 kinase. *Circulation*. 2009; 120:2077–2087. [PubMed: 19901187]
14. Mohsin S, Khan M, Toko H, et al. Human cardiac progenitor cells engineered with Pim-I kinase enhance myocardial repair. *J Am Coll Cardiol*. 2012; 60:1278–1287. [PubMed: 22841153]
15. Choudhery MS, Khan M, Mahmood R, Mohsin S, Akhtar S, Ali F, Khan SN, Riazuddin S. Mesenchymal stem cells conditioned with glucose depletion augments their ability to repair-infarcted myocardium. *J Cell Mol Med*. 2012; 16:2518–2529. [PubMed: 22435530]
16. Zippo A, De Robertis A, Bardelli M, Galvagni F, Oliviero S. Identification of Flk-1 target genes in vasculogenesis: Pim-1 is required for endothelial and mural cell differentiation in vitro. *Blood*. 2004; 103:4536–4544. [PubMed: 14982870]
17. Borillo GA, Mason M, Quijada P, et al. Pim-1 kinase protects mitochondrial integrity in cardiomyocytes. *Circ Res*. 2010; 106:1265–1274. [PubMed: 20203306]
18. Din S, Mason M, Völkers M, Johnson B, Cottage CT, Wang Z, Joyo AY, Quijada P, Erhardt P, Magnuson NS, Konstandin MH, Sussman MA. Pim-1 preserves mitochondrial morphology by inhibiting dynamin-related protein 1 translocation. *Proc Natl Acad Sci U S A*. 2013; 110:5969–5974. [PubMed: 23530233]
19. Yan B, Zemskova M, Holder S, Chin V, Kraft A, Koskinen PJ, Lilly M. The PIM-2 kinase phosphorylates BAD on serine 112 and reverses BAD-induced cell death. *J Biol Chem*. 2003; 278:45358–45367. [PubMed: 12954615]
20. Willeit P, Willeit J, Brandstätter A, Ehrlenbach S, Mayr A, Gasperi A, Weger S, Oberhollenzer F, Reindl M, Kronenberg F, Kiechl S. Cellular aging reflected by leukocyte telomere length predicts advanced atherosclerosis and cardiovascular disease risk. *Arterioscler Thromb Vasc Biol*. 2010; 30:1649–1656. [PubMed: 20508208]
21. Fyhrquist F, Saijonmaa O, Strandberg T. The roles of senescence and telomere shortening in cardiovascular disease. *Nat Rev Cardiol*. 2013; 10:274–283. [PubMed: 23478256]
22. Moslehi J, DePinho RA, Sahin E. Telomeres and mitochondria in the aging heart. *Circ Res*. 2012; 110:1226–1237. [PubMed: 22539756]
23. Alt EU, Senst C, Murthy SN, Slakey DP, Dupin CL, Chaffin AE, Kadowitz PJ, Izadpanah R. Aging alters tissue resident mesenchymal stem cell properties. *Stem Cell Res*. 2012; 8:215–225. [PubMed: 22265741]
24. Cawthon RM. Telomere length measurement by a novel monochrome multiplex quantitative PCR method. *Nucleic Acids Res*. 2009; 37:e21. [PubMed: 19129229]
25. Cottage CT, Neidig L, Sundararaman B, Din S, Joyo AY, Bailey B, Gude N, Hariharan N, Sussman MA. Increased mitotic rate coincident with transient telomere lengthening resulting from pim-1 overexpression in cardiac progenitor cells. *Stem Cells*. 2012; 30:2512–2522. [PubMed: 22915504]
26. Capogrossi MC. Cardiac stem cells fail with aging: a new mechanism for the age-dependent decline in cardiac function. *Circ Res*. 2004; 94:411–413. [PubMed: 15001538]
27. Cesselli D, Beltrami AP, D'Aurizio F, et al. Effects of age and heart failure on human cardiac stem cell function. *Am J Pathol*. 2011; 179:349–366. [PubMed: 21703415]
28. Dimmeler S, Leri A. Aging and disease as modifiers of efficacy of cell therapy. *Circ Res*. 2008; 102:1319–1330. [PubMed: 18535269]
29. Lakatta EG. Arterial and cardiac aging: major shareholders in cardiovascular disease enterprises: part III: cellular and molecular clues to heart and arterial aging. *Circulation*. 2003; 107:490–497. [PubMed: 12551876]
30. De Angelis A, Piegari E, Cappetta D, Marino L, Filippelli A, Berrino L, Ferreira-Martins J, Zheng H, Hosoda T, Rota M, Urbanek K, Kajstura J, Leri A, Rossi F, Anversa P. Anthracycline cardiomyopathy is mediated by depletion of the cardiac stem cell pool and is rescued by restoration of progenitor cell function. *Circulation*. 2010; 121:276–292. [PubMed: 20038740]

31. Lakatta EG, Levy D. Arterial and cardiac aging: major shareholders in cardiovascular disease enterprises: Part I: aging arteries: a “set up” for vascular disease. *Circulation*. 2003; 107:139–146. [PubMed: 12515756]
32. Leri A, Franco S, Zacheo A, Barlucchi L, Chimenti S, Limana F, Nadal-Ginard B, Kajstura J, Anversa P, Blasco MA. Ablation of telomerase and telomere loss leads to cardiac dilatation and heart failure associated with p53 upregulation. *EMBO J*. 2003; 22:131–139. [PubMed: 12505991]
33. Leri A, Barlucchi L, Limana F, Deptala A, Darzynkiewicz Z, Hintze TH, Kajstura J, Nadal-Ginard B, Anversa P. Telomerase expression and activity are coupled with myocyte proliferation and preservation of telomeric length in the failing heart. *Proc Natl Acad Sci USA*. 2001; 98:8626–8631. [PubMed: 11447262]
34. Mohsin S, Siddiqi S, Collins B, Sussman MA. Empowering adult stem cells for myocardial regeneration. *Circ Res*. 2011; 109:1415–1428. [PubMed: 22158649]
35. Lakatta EG. Cardiovascular regulatory mechanisms in advanced age. *Physiol Rev*. 1993; 73:413–467. [PubMed: 8475195]
36. Chimenti C, Kajstura J, Torella D, Urbanek K, Heleniak H, Colussi C, Di Meglio F, Nadal-Ginard B, Frustaci A, Leri A, Maseri A, Anversa P. Senescence and death of primitive cells and myocytes lead to premature cardiac aging and heart failure. *Circ Res*. 2003; 93:604–613. [PubMed: 12958145]
37. Bishopric NH. A longer, better ride with engineered stem cells. *J Am Coll Cardiol*. 2012; 60:1288–1290. [PubMed: 22841152]
38. Rota M, LeCapitaine N, Hosoda T, et al. Diabetes promotes cardiac stem cell aging and heart failure, which are prevented by deletion of the p66shc gene. *Circ Res*. 2006; 99:42–52. [PubMed: 16763167]

## Novelty and Significance

### What Is Known?

- Aging and disease compromise cardiac progenitor cell (CPC) function.
- Pim-1 modification of CPCs enhances survival, proliferation, and lineage commitment capacity of adoptively transferred CPCs, improving myocardial regeneration after infarction.

### What New Information Does This Article Contribute?

- CPCs isolated from multiple patients exhibit differences in growth kinetics and telomere length consistent with biological aging.
- Pim-1 modification rejuvenates aged and diseased CPC pool by increasing telomere length and decreasing cell cycle inhibitors.
- Beneficial effects of Pim-1 modification are more pronounced in human CPCs with slow-growth kinetics.

Myocardial regeneration and repair mediated by human CPCs is compromised by biological aging. Impairment of CPCs function is further accelerated by chronic stress or disease conditions. Here, we report that human adult CPCs isolated from multiple patients with heart failure undergoing left ventricular assist device implantation vary with respect to growth kinetics, all of which were inferior when compared with human fetal CPCs. Fetal CPCs were used as a gold standard in the study intended to represent a highly cardiogenic cell that would be ideal to promote cardiomyogenesis and myocardial repair. Pim-1 modification of human adult CPCs reversed their senescent phenotype as evidenced by lengthening of the telomeres, improved growth kinetics, and delayed replicative senescence. Genetic engineering with Pim-1 modification was beneficial for all CPCs tested although CPCs with slow-growth kinetics benefited the most by restoration of youthful phenotypic characteristics. Therefore, the efficacy of CPC transfer therapy is expected to be improved by Pim-1 modification that rejuvenates CPCs impaired by age and chronic disease. The ability of Pim-1 modification to rejuvenate compromised CPCs may enable stem cell treatment availability to patients currently considered as poor candidates for therapeutic intervention because of advanced age or chronic comorbidities presenting together with heart failure.

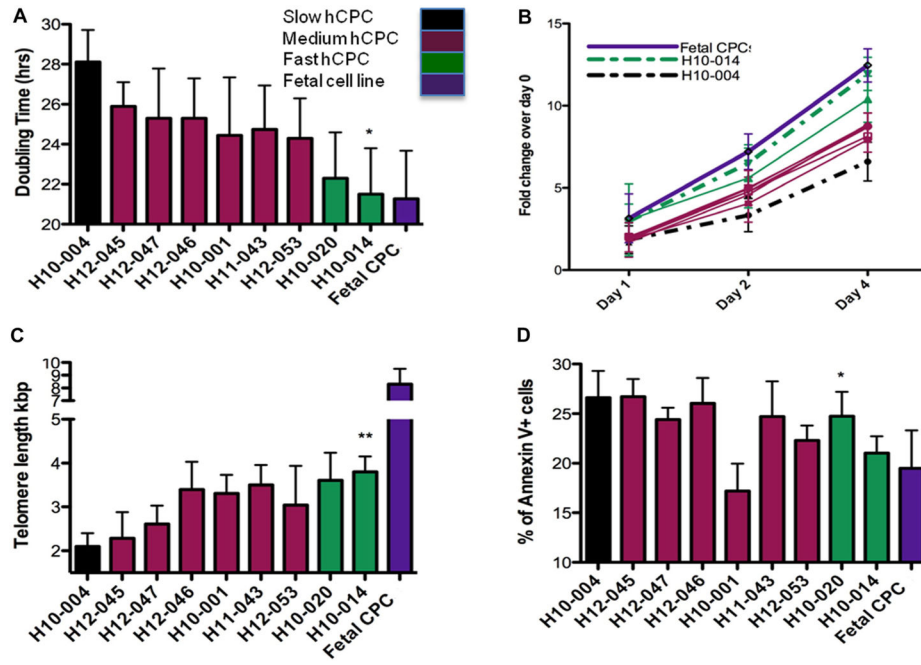


**Figure 1. Characterization of human cardiac progenitor cell (hCPC) isolated from multiple patients**

**A**, hCPCs show variation in population doubling times as measured by CyQuant and viability assay cell counts from multiple patients (n=3). **B**, Differences in proliferation rates are observed in multiple hCPC lines (n=3). **C**, Telomere lengths in multiple hCPC lines show variability as measured by real-time polymerase chain reaction (n=6). **D**, Percentage of dead cells measured by Annexin-V staining showed variability in multiple hCPC lines when exposed to 30  $\mu\text{mol/L}$  of  $\text{H}_2\text{O}_2$  challenge (n=3). Black bar represents hCPC with slow-growth kinetics (hCPC-S), maroon bars represents hCPC with medium growth kinetics, green bars represents hCPC with fast-growth kinetics (hCPC-F), purple bar represent hCPC isolated from fetal heart samples (Fetal CPC).

\* $P < 0.05$ , \*\* $P < 0.01$ . Significance values are calculated for hCPC-S versus hCPC-F groups.

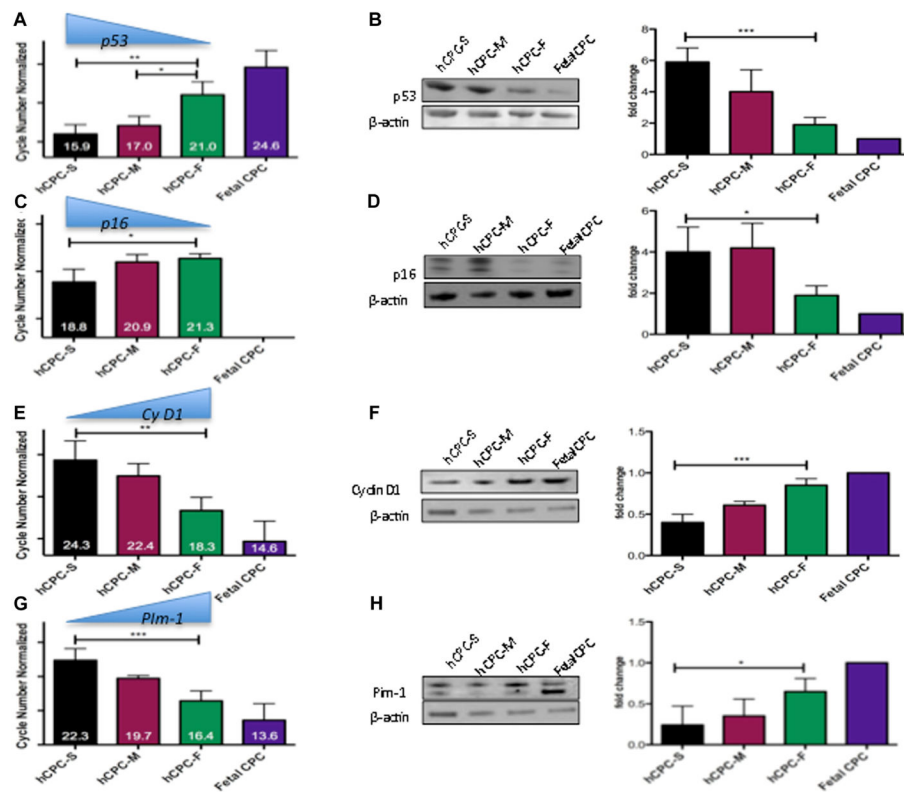


**Figure 2. Growth kinetics profiling in multiple human cardiac progenitor cells (hCPC) lines**

**A** and **C**, mRNA levels of senescence-associated markers p53 and p16 are upregulated in hCPC with slow-growth kinetics (hCPC-S) as compared with hCPC with fast-growth kinetics (hCPC-F) measured by real-time polymerase chain reaction (n=4), data are represented as cycle numbers normalized to 18S (Ct values are inversely proportional to gene expression (ie, lower cycle number corresponds to higher mRNA expression)). **E** and **G**, Proliferative markers Cyclin D1 and Pim-1 are upregulated in hCPC-F compared with hCPC-S (n=4), data are represented as cycle numbers normalized to 18S (Ct values are inversely proportional to gene expression), **B**, **D**, **F**, and **H**, Immunoblot analysis for p53, p16, Cyclin D1, and Pim-1, respectively (n=3) with graphical representation in fold change over Fetal hCPC (each sample is normalized to  $\beta$ -actin) \* $P$ <0.05, \*\* $P$ <0.01, \*\*\* $P$ <0.001. Black bar represents hCPC with slow-growth kinetics (hCPC-S), maroon bars represents hCPC with medium growth kinetics (hCPC-M), green bars represents hCPC with fast-growth kinetics (hCPC-F), purple bar represents hCPC isolated from fetal heart samples (Fetal CPC). Significance values are calculated for hCPC-S vs hCPC-F.

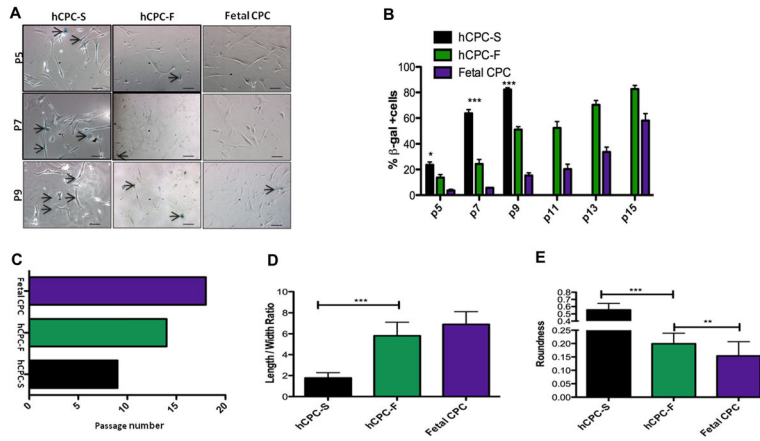


**Figure 3. Replicative senescence in human cardiac progenitor cells (hCPC)**

**A**, Senescence-associated β-galactosidase staining in hCPC with slow-growth kinetics (hCPC-S), hCPC with fast-growth kinetics (hCPC-F), and Fetal CPC at increasing passage numbers. Arrows indicate blue senescent cells positive for β-galactosidase staining. **B**, Percentage of β-galactosidase-positive cells in hCPC-S, hCPC-F, Fetal CPC after subsequent passaging. **C**, Graphical representation of passage numbers indicating growth arrest in hCPC-S, hCPC-F, and Fetal CPC to induce replicative senescence. **D** and **E**, Decrease in cell length:width ratio and increase in roundness is observed in hCPC-S compared with hCPC-F at passage 9. \* $P < 0.05$ , \*\* $P < 0.01$ , \*\*\* $P < 0.001$ . Black bar represents hCPC-S, green bars represents hCPC-F, purple bar represents Fetal CPC. Significance values are calculated for hCPC-S vs hCPC-F groups. Scale bar represents 100 μm.

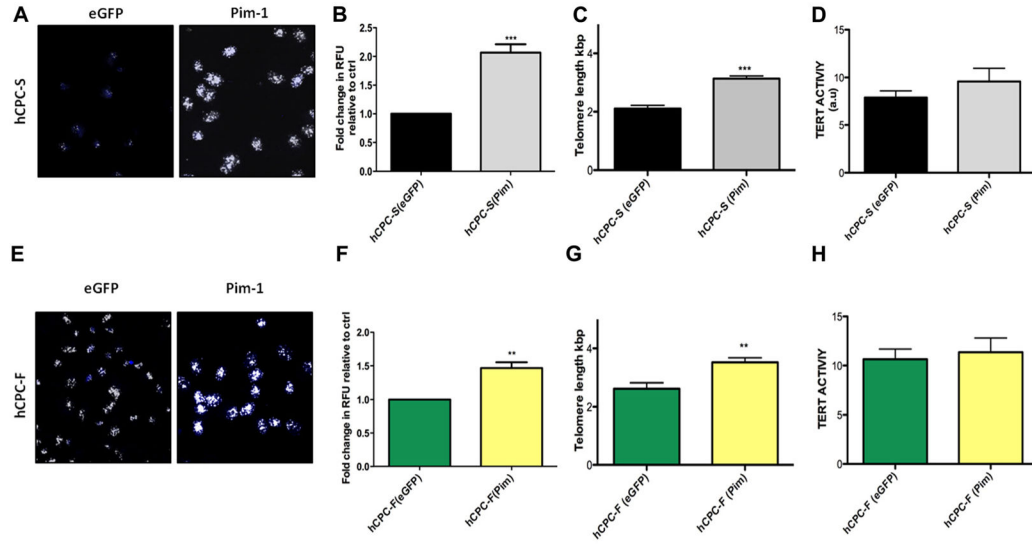


**Figure 4. Increased telomere length and telomerase activity after Pim-1 modification**

**A** and **E**, Confocal micrographs of telomere staining assessed by quantitative fluorescence in situ hybridization in hCPC with slow-growth kinetics (hCPC-S) and hCPC with fast-growth kinetics (hCPC-F), respectively, white foci indicate telomere staining; blue staining represents nuclei stained with sytox blue (n=3). **B** and **F**, Quantitation of telomere length performed by measuring relative fluorescent unit (RFU) by confocal microscope in hCPC-S and hCPC-F relative to their respective enhanced green fluorescent protein (eGFP) controls (n=3; ~100 cells are included per group). **C** and **G**, Increased telomere lengths are observed in hCPC after Pim-1 modification measured by real-time polymerase chain reaction analysis (n=6). **D** and **H**, Tert activity measured by TRAPEze assay (n=3) measured in hCPC-S (Pim-1) and hCPC-F (Pim-1) relative to their respective eGFP control hCPC and expressed as arbitrary unit (a.u.). \* $P < 0.05$ , \*\* $P < 0.01$ , \*\*\* $P < 0.001$ . Significance values are calculated for eGFP vs Pim in both hCPC groups.

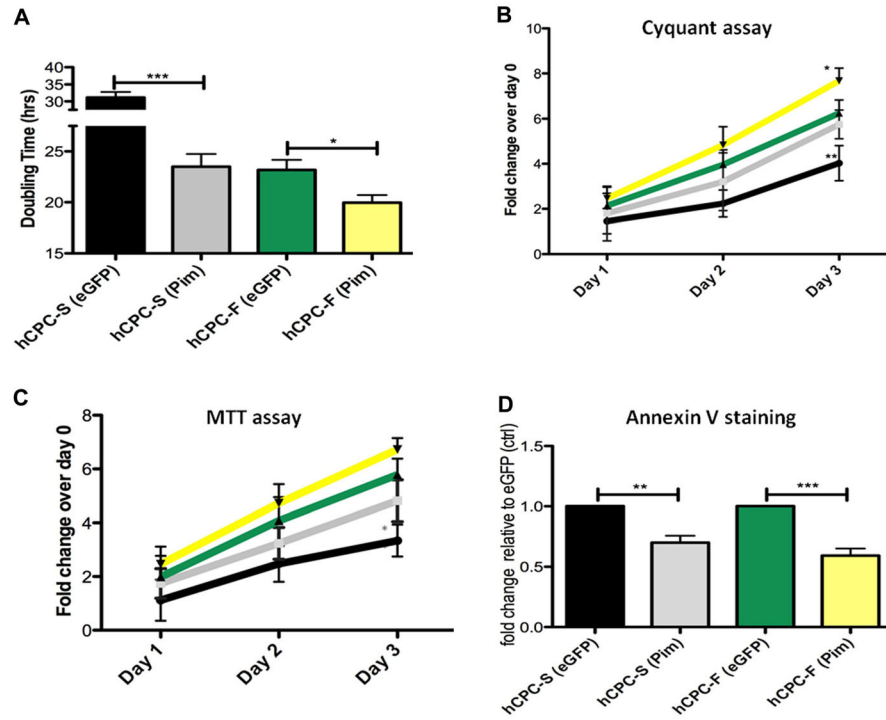


**Figure 5. Enhanced proliferation, metabolic activity, and survival after Pim-1 modification of human cardiac progenitor cells (hCPCs) with fast- and slow-growth kinetics (hCPC-F and hCPC-S, respectively)**

**A**, Increased population doubling time calculated by CyQuant and viability assay cell counts after Pim-1 modification (n=3). **B** and **C**, Increased proliferation rate and metabolic activity in genetically modified hCPC-S and hCPC-F with Pim-1 (n=3). **D**, Percentage of Annexin-V+ cells are measured by fluorescence activated cell sorting analysis after apoptotic stimuli of 30  $\mu\text{mol/L}$   $\text{H}_2\text{O}_2$  shows increased cell survival after Pim-1 modification (n=3). \* $P < 0.05$ , \*\* $P < 0.01$ , \*\*\* $P < 0.001$ . Significance values are calculated for enhanced green fluorescent protein (eGFP) vs Pim in both hCPC groups.

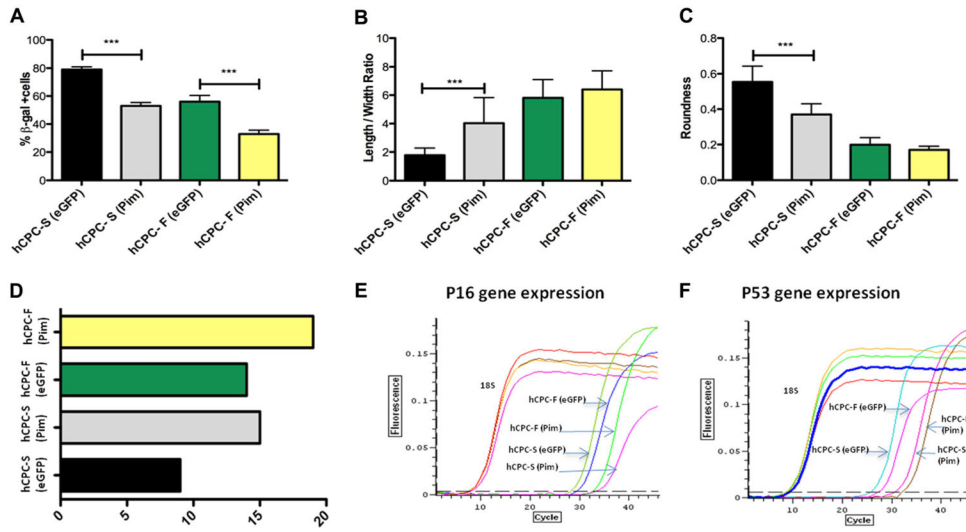


**Figure 6. Pim-1 ameliorates human cardiac progenitor cell (hCPC) senescence**

**A**, Percentage of senescence-associated β-galactosidase-positive cells in hCPC modified with Pim-1 at passage 9. **B** and **C**, Length:width ratio and roundness of hCPC show well-maintained normal morphology after Pim-1 modification measured by ImageJ software. **D**, Graphical representation of passage numbers indicating growth arrest in hCPC with slow-growth kinetics (hCPC-S; Pim-1), and hCPC with fast-growth kinetics (hCPC-F; Pim-1) after replicative senescence. **E** and **F**, Decrease in expression of senescence-associated markers measured by p16 and p53 gene expression after Pim-1 modification (n=3) \*\*\**P*<0.001. Significance values are calculated for GFP expressing vs Pim in both hCPC groups.

**Table 1**

**Table Clinical Profile of Patients Used for hCPC Cell Isolation**

Patient ID	Age, y	Sex	Growth Rate Relative to Fetal CPC, %	EF%	Cardiac Index	Diabetes Mellitus	Hyperlipidemia	Smoking	Infarct	Ischemia	ACE Inhibitor	$\beta$ -Blocker	Anticoagulant	NYHA
H10-004; hCPC-S	82	Male	-18.9	8	2		1 Pk/d for 30 y	Multiple			x	x	Aspirin	IV
H12-045	75	Male	-13.5	19	2.4	x		x			x	x	Aspirin	IV
H12-047	72	Male	-10.9	8	1.1		x	x	x	x	x	x	Aspirin	IV
H12-046	47	Male	-10.9	20	1.3	x	x	x	x	x	x	x	Aspirin	IV
H10-001	68	Male	-8.5	11	1.6		x	x	x	x	x	x	Aspirin	IV
H11-043	42	Male	-7.0	20	1.6			x	x	x	x		Aspirin	IV
H12-053	61	Male	-8.6	15	1.75			x					Aspirin	IV
H11-020	68	Male	-5.9	20	1.7	x	x	x	x	x	x	x	Aspirin	IV
H10-014; hCPC-F	73	Male	-5.7	17	1.6	x	x	. but stopped 25 y ago	Multiple with recent cardiogenic shock		x	x	Aspirin	IV

EF indicates ejection fraction; hCPC, human cardiac progenitor cells; hCPC-F, hCPC with fast-growth kinetics; hCPC-S, hCPC with slow-growth kinetics; and NYHA, New York Heart Association.